JACS
JOURNAL OF THE AMERICAN CHEMICAL SOCIETY
Article
pubs.acs.org/JACS

Systematic Analyses of Substrate Preferences of 20S Proteasomes Using Peptidic Epoxyketone Inhibitors

Eva M. Huber,[†,∥] Gerjan de Bruin,[‡,∥] Wolfgang Heinemeyer,[†] Guillem Paniagua Soriano,[‡] Herman S. Overkleeft,*[,‡] and Michael Groll*[,†]

[†]Center for Integrated Protein Science at the Department Chemie, Lehrstuhl für Biochemie, Technische Universität München, 85748 Garching, Germany

[‡]Gorlaeus Laboratories, Leiden Institute of Chemistry and Netherlands Proteomics Center, Einsteinweg 55, 2333 CC Leiden, The Netherlands

Supporting Information

ABSTRACT: Cleavage analyses of 20S proteasomes with natural or synthetic substrates allowed to infer the substrate specificities of the active sites and paved the way for the rational design of high-affinity proteasome inhibitors. However, details of cleavage preferences remained enigmatic due to the lack of appropriate structural data. In a unique approach, we here systematically examined substrate specificities of yeast and human proteasomes using irreversibly acting α',β'epoxyketone (ep) inhibitors. Biochemical and structural analyses provide unique insights into the substrate preferences of the distinct active sites and highlight differences between proteasome types that may be considered in future inhibitor design efforts. (1) For steric reasons, epoxyketones with Val or Ile at the P1 position are weak inhibitors of all active sites. (2) Identification of the β2c selective compound Ac-LAE-ep represents a promising starting point for the development of compounds that discriminate between β2c and β2i. (3) The compound Ac-LAA-ep was found to favor subunit β5c over β5i by three orders of magnitude. (4) Yeast β1 and human β1c subunits preferentially bind Asp and Leu in their S1 pockets, while Glu and large hydrophobic residues are not accepted. (5) Exceptional structural features in the β1/2 substrate binding channel give rise to the β1 selectivity of compounds featuring Pro at the P3 site. Altogether, 23 different epoxyketone inhibitors, five proteasome mutants, and 43 crystal structures served to delineate a detailed picture of the substrate and ligand specificities of proteasomes and will further guide drug development efforts toward subunit-specific proteasome inhibitors for applications as diverse as cancer and autoimmune disorders.

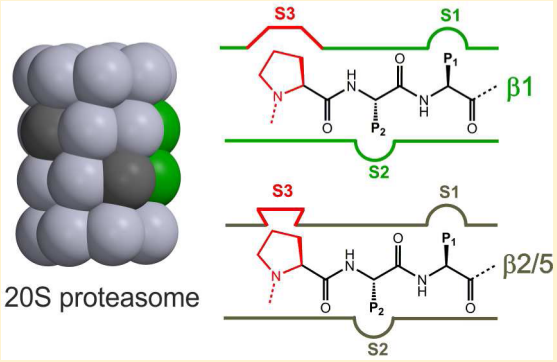

INTRODUCTION

The majority of intracellular protein degradation in eukaryotes is mediated by the 20S proteasome core particle (CP). While yeast expresses only one type of proteasome (yCP), divergent evolution endowed vertebrates with three distinct CPs that differ in their subunit compositions, substrate specificity, and biological significance: the constitutive proteasome (cCP: active sites β1c, β2c, β5c), the immunoproteasome (iCP: β1i, β2i, β5i), and the thymoproteasome (tCP: β1i, β2i, β5t).[1,2] With their three different proteolytic centers, CPs can cleave polypeptides after virtually all amino acids.[3] The trypsin-like (T-L) active sites, residing in the β2 subunits, preferentially cut substrates after positively charged residues. This cleavage specificity is strictly conserved among eukaryotes and between CP types, thus making it highly challenging to design β2c- or β2i-specific inhibitors.[4] The β5 active sites exert the most important chymotrypsin-like (ChT-L) activity (processing after hydrophobic residues) by accommodating apolar amino acids in their S1 specificity pocket. In contrast, substrate cleavage preferences between β1 subunits of yCP/cCP and iCP significantly differ.[5,6] The hydrophilic nature of the yβ1 and β1c active sites promotes the hydrolysis of peptide bonds C-terminally of acidic amino acids (peptidylglutamyl-peptide hydrolyzing (PGPH)[7] or caspase-like (C-L)[8] activity), whereas the more hydrophobic lining of the β1i active site of iCPs is optimized to generate peptides with hydrophobic C-termini for immune surveillance.[3,6] These cleavage specificities, which have mostly been investigated by activity assays with natural or synthetic model substrates,[5,8−12] served as guidelines for the development of proteasome inhibitors. However, the design of subunit-selective compounds, which represent valuable tools to evaluate the contribution of the individual active sites to antigen processing and to diseases like autoimmune disorders and cancer, requires a more detailed understanding of proteasome substrate specificities. We therefore synthesized 18 tripeptide α',β'epoxyketone inhibitors[13] featuring Leu or Pro in P3, Ala or Leu in P2, and distinct side chains in P1. Binding preferences

Received: April 9, 2015
Published: May 28, 2015

DOI: 10.1021/jacs.5b03688
J. Am. Chem. Soc. 2015, 137, 7835−7842

and IC_{50} values for the human cCP and iCP subunits were determined by competitive activity based protein profiling (ABPP) in Raji cell lysates and for purified yCPs by fluorogenic substrate assays. A separate series of five inhibitors was used to assess inhibition of $\beta1$ depending on the presence or absence of a P4 site.[8] X-ray crystallographic analyses of all compounds in complex with the yCP together with yeast mutagenesis uncover unexpected and interesting aspects of the proteasomal substrate specificity.

RESULTS AND DISCUSSION

Choice of Employed Organisms, Proteasome Inhibitor Types, and Assay Setup. Despite recent progress,[6,14] mouse and human CPs are still difficult to crystallize and not suitable for extensive structural analyses with various ligands. We therefore used the yCP for our crystallographic and mutagenesis studies. The conserved fold of proteasome subunits and the identical binding mode of peptidic compounds to yeast and mammalian CPs justify usage of the model system yeast.[6] Active yCP crystals were soaked with final ligand concentrations of 3.3 mM. At this concentration, even poor inhibitors bind to the active sites of the yCP and thus can be visualized by X-ray crystallography. Biochemical data were determined for yeast and human samples in separate experimental set-ups. Inhibitors were incubated for 1 h with human Raji cell lysate or purified yeast CP. Subsequently, blockage of human CPs was analyzed by determining residual proteasome activity with fluorescently labeled activity based probes (Figure 2d; Figure S1a, Supporting Information),[15,16] whereas inhibition of the yCP was determined by measuring the residual proteasome activity after the addition of subunit-specific 7-amino-4-methylcoumarin (AMC)-substrates (Figure 2c; Figure S1b, Supporting Information). All synthesized inhibitors share the α',β'epoxyketone (ep) warhead, which afforded us to use carfilzomib and ONX 0914 as reference compounds. Although distinct covalent inhibitor types[17] and natural substrates may slightly vary in their binding mode to the S pockets of the proteasomal active site (Figure 1), the analyses provided here disclose significant tendencies for substrate preferences.

Epoxyketones with P1-Valine or -Isoleucine Are Weak Proteasome Inhibitors. Among the different P1 residues tested (Table 1; Table S1, Supporting Information), Val and Ile are the most disfavored ones (IC_{50} for human CP $\geq$ 7.2 μM, for yCP $\geq$ 100 μM; Tables 2 and 3; Tables S2–S4, Supporting Information). For example, the compounds Ac-LAI-ep ($\geq$8.1 μM) and Ac-LAV-ep ($\geq$7.2 μM) are significantly less potent for human CPs than Ac-LAL-ep ($\leq$1 μM). The conformation of Val and Ile in the S1 pocket clearly differs from that observed for Leu. Val and Ile are sandwiched in the S1 pocket between the main chain heteroatoms 19O, 45O, 47O, and 47N (Figure S2, Supporting Information). On the basis of the interatomic distances, we postulate that also Thr is disfavored at the P1 position, but experimental support for this hypothesis is lacking due to the abortive synthesis of the respective epoxyketones.

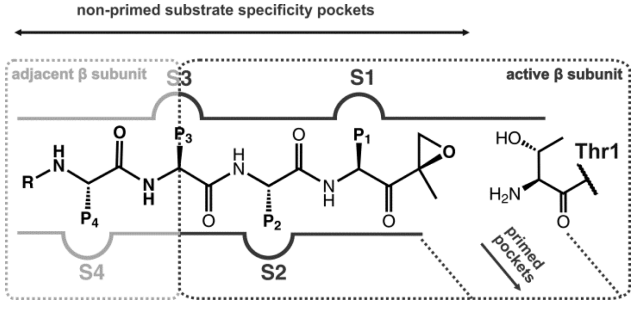

Figure 1. Proteasomal substrate binding channel. Each active site is formed by two neighboring subunits. The reactive β subunit, harboring the catalytic Thr1, forms the primed substrate binding channel and the non-primed S1, S2, and S3 pockets. The adjacent β subunit contributes to the S3 pocket and is engaged in binding of P4 residues.

Table 1. Chemical Structures of Synthesized Compounds

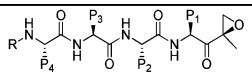

Compound	R	P4	P3	P2	P1
Ac-PAD-ep		-			
Ac-LAD-ep		-			
Ac-PAE-ep		-			
Ac-LAE-ep		-			
Ac-PAF-ep		-			
Ac-LAF-ep		-			
Ac-PAY-ep		-			
Ac-LAY-ep		-			
Ac-PAI-ep		-			
Ac-LAI-ep		-			
Ac-PAL-ep		-			
Ac-LAL-ep		-			
Ac-PAV-ep		-			
Ac-LAV-ep		-			
Ac-PAA-ep		-			
Ac-LAA-ep		-			
Ac-PLL-ep		-			
Ac-LLL-ep		-			
H-APLL-ep	H				
Ac-APLL-ep					
N_3G-APAL-ep					
N_3G-APnLL-ep					
N_3G-A(4,4-F_2P)nLL-ep					

Blockage of $\beta2$ Subunits. The marginal structural differences between the $\beta2$c and $\beta2$i subunits (Asp53 ($\beta2$c) versus Glu53 (y$\beta2$/$\beta2$i) and Thr48 (y$\beta2$/$\beta2$c) versus Val48 ($\beta2$i)) do not provide an obvious explanation for the biological need of their mutual exchange in mammalian CPs[6] and complicate the design of $\beta2$c- and $\beta2$i-selective inhibitors.[4] To

DOI: 10.1021/jacs.5b03688
J. Am. Chem. Soc. 2015, 137, 7835–7842

Table 2. IC_{50} Values [μM] of Compounds As Determined by ABPP with Raji Cell Lysates

compound	β1c	β1i	β2c	β2i	β5c	β5i
Ac-PAD-ep	1.4	>1000	>1000	>1000	>1000	>1000
Ac-LAD-ep	1.6	>1000	115	226	21.7	12.3
Ac-PAE-ep	17.7	>1000	>1000	>1000	>1000	>1000
Ac-LAE-ep	14.8	>1000	3.6	106	>1000	>1000
Ac-PAF-ep	10.8	0.021	540	625	5.5	2.1
Ac-LAF-ep	61.7	0.23	0.55	0.78	0.02	0.11
Ac-PAY-ep	10.3	0.38	69.0	65.1	4.9	1.5
Ac-LAY-ep	5.3	0.33	0.14	0.14	0.054	0.15
Ac-PAI-ep	338	28.9	>1000	>1000	>1000	>1000
Ac-LAI-ep	261	10.8	9.2	8.1	19.7	253
Ac-PAL-ep	0.11	0.028	326.7	446.6	9.5	10.7
Ac-LAL-ep	0.95	0.020	0.083	0.074	0.06	1.0
Ac-PAV-ep	>1000	36.0	>1000	>1000	≈1000	>1000
Ac-LAV-ep	>1000	101.5	7.2	15.6	25.9	≈1000
Ac-PAA-ep	>1000	99.5	457	432	248	>1000
Ac-LAA-ep	>100	26.8	1.4	2.8	1.1	>1000
Ac-PLL-ep	0.11	0.040	93.2	46.4	10.8	8.8
Ac-LLL-ep	0.14	0.015	0.041	0.017	0.1	1.0
H-APLL-ep	0.72	0.085	61.5	160	21.9	131
Ac-APLL-ep	0.029	0.035	75.1	37.3	26.6	52.4
N_3G-APAL-ep	0.20	0.043	>1000	>1000	43.8	46.2
N_3G-APnLL-ep	0.067	0.026	>100	>100	≈100	≈100
N_3G-A(4,4-F_2P)nLL-ep	2.7	0.031	>100	>100	6.2	17.1
carfilzomib	0.075	0.017	0.031	0.017	0.00089	0.0013
ONX 0914[18]	>10	0.46	1.1	0.59	0.054	0.0057
bortezomib	0.017	0.0065	0.51	0.57	0.0027	0.0027

Table 3. IC_{50} Values [μM] of Compounds for Purified wt yCP

compound	yβ1	yβ2	yβ5
Ac-PAD-ep	22.37 ± 1.29	>200	>200
Ac-LAD-ep	24.46 ± 1.78	>200	~100
Ac-PAE-ep	>200	>200	~200
Ac-LAE-ep	>200	>200	~200
Ac-PAF-ep	>200	>200	10.91 ± 1.18
Ac-LAF-ep	>200	10.00 ± 1.01	0.23 ± 0.03
Ac-PAY-ep	>200	>200	7.91 ± 0.89
Ac-LAY-ep	>200	6.04 ± 0.69	0.27 ± 0.04
Ac-PAI-ep	>200	>200	>200
Ac-LAI-ep	>200	>200	100.4 ± 12.5
Ac-PAL-ep	43.34 ± 2.12	>200	>200
Ac-LAL-ep	55.50 ± 2.18	14.42 ± 1.03	0.67 ± 0.08
Ac-PAV-ep	>200	>200	>200
Ac-LAV-ep	>200	>200	>200
Ac-PAA-ep	>200	>200	>200
Ac-LAA-ep	>200	65.80 ± 10.96	89.25 ± 11.33
Ac-PLL-ep	39.76 ± 6.32	>200	~200
Ac-LLL-ep	40.94 ± 2.67	10.36 ± 1.89	0.72 ± 0.08
H-APLL-ep	101.1 ± 11.68	>200	>200
Ac-APLL-ep	10.32 ± 1.36	>200	~200
N_3G-APAL-ep	7.59 ± 0.52	>200	>200
N_3G-APnLL-ep	5.32 ± 0.39	>200	~200
N_3G-A(4,4-F_2P)nLL-ep	11.39 ± 0.76	>200	>200
carfilzomib	~200	1.80 ± 0.51	0.03 ± 0.02
ONX 0914	>200	5.48 ± 0.49	0.42 ± 0.05
bortezomib	1.07 ± 0.05	9.33 ± 1.42	0.05 ± 0.02

gain additional insights into the β2 substrate specificities, we tested our compounds for blockage of the T-L activities. Ligands bearing Pro at P3 poorly inhibit the β2 active sites of yeast and human CPs, while P3-Leu analogues are much more potent (up to 6000 times). Among the P3-Leu series, inhibitors with Leu, Phe, and Tyr at P1 display highest affinities and do not discriminate between the human c- and i-subunits (Tables 2 and 3). These results confirm that the β2 subunits accept

DOI: 10.1021/jacs.5b03688
J. Am. Chem. Soc. 2015, 137, 7835−7842

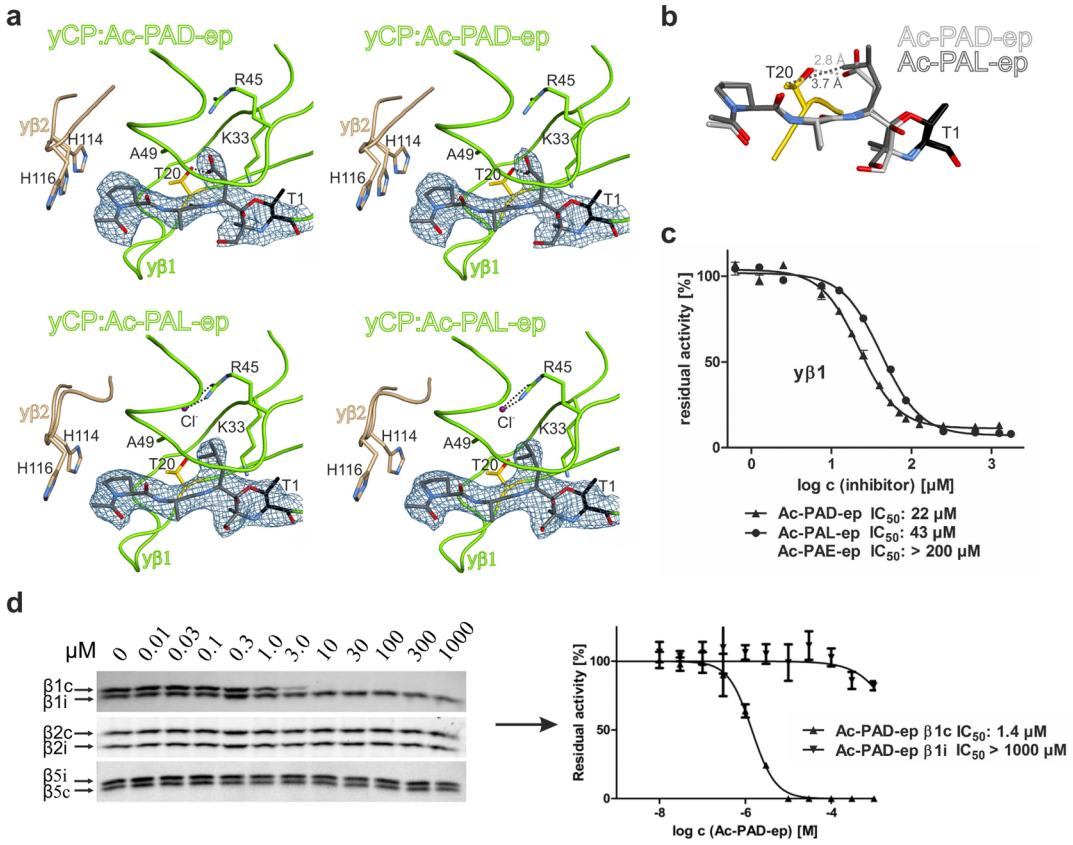

Figure 2. Yeast β1 active site favors Asp or Leu in its S1 pocket. (a) Stereo illustration of the $2F_O - F_C$ electron density map (blue mesh; contoured at 1σ) for Ac-PAD-ep (upper panel) and Ac-PAL-ep (lower panel) bound to the yβ1 active site (green) of the wt yeast 20S proteasome (yCP). The active site Thr1 is marked in black, Thr20 in yellow. The chloride ion is depicted as a purple sphere. Hydrogen bonds are indicated by black dashed lines. Important residues of the neighboring subunit yβ2 (brown), contributing to the S3 and S4 pockets of the yβ1/yβ2 substrate binding channel, are illustrated. His114 adopts alternative conformations. Amino acids are labeled by the one-letter code and numbered according to the sequence alignment to the proteasomal β subunit of *Thermoplasma acidophilum*.[24] (b) Structural superposition of Ac-PAD-ep and Ac-PAL-ep in their yβ1-bound conformations. Note the distinct orientations of the ligands' P1 residues. Thr20OH is hydrogen-bonded to the P1-Asp residue of Ac-PAD-ep (light gray; distance 2.8 Å), while the P1-Leu side chain of Ac-PAL-ep undergoes hydrophobic contacts with the methyl group of Thr20 (dark gray; distance 3.7 Å). (c) Purified wt yCPs were tested for inhibition of their C-L activity (yβ1) by Ac-PAD-ep, Ac-PAL-ep, and Ac-PAE-ep using the substrate Z-LLE-AMC. Inhibitors were incubated with yCP for 1 h at room temperature; IC_{50} values were determined in triplicates; standard deviations are indicated by bars. (d) ABPP inhibition profile of Ac-PAD-ep in Raji cell lysate. The inhibitor and the cell lysate were incubated for 1 h at 37 °C and probed with azido-boron-dipyrromethene (BODIPY)-MeTyr-Phe-Leu-vinyl sulfone (0.1 μM; to probe β5) or a mixture of BODIPY-epoxomicin (0.5 μM; to probe all subunits, used for β2-profiling) and BODIPY-FL-Ala-Pro-Nle-Leu-ep (0.25 μM; to probe β1 activity). Upon separation on SDS-PAGE and in-gel fluorescent detection (left), band quantification provided inhibition curves (right), from which IC_{50} values were derived.

nonpolar P1 side chains[3] besides basic ones such as Arg.[4] Small P1 residues like Ala, however, are less potent due to the large S1 pockets of β2 subunits. The acidic amino acids Asp and Glu are also hardly effective toward yeast and human CPs, except for Ac-LAE-ep, which selectively targets the human β2c subunit (IC_{50}: 3.6 μM; Table 2). In contrast to β2i, where Glu53 is oriented toward His35, Asp53O$^{\delta}$ of β2c may hydrogen-bond to the P1-Glu side chain of the ligand via a solvent molecule, thereby enhancing the affinity of Ac-LAE-ep for β2c compared to β2i (IC_{50}: 106 μM; Table 2) by a factor of 30.[6,14]

Inhibition of Subunit β5. Characterization of the β5 substrate binding channel by numerous natural and synthetic ligands revealed that the S3 pockets of yeast and mammalian β5 subunits readily accept Leu residues.[14,19] We tested the impact of Leu versus Pro at the P3 site and found that the latter is not suitable to target the ChT-L activity (up to 300 times decreased potency compared to P3-Leu inhibitors). Yeast β5 and mammalian constitutive β5c subunits lack a defined S2 pocket[3,6,14] (Gly48), and consequently, exchange of the P2-Ala by Leu does not significantly affect IC_{50} values. For instance, the compounds Ac-LAL-ep and Ac-LLL-ep as well as Ac-PAL-ep and Ac-PLL-ep are equipotent (Tables 2 and 3). Nonetheless, potency and subunit selectivity may be affected by larger P2 side chains such as Phe, Tyr, or Trp, which provide additional anchorage especially in subunit β5i by interacting with Cys48.[6]

Proteasomal β5 subunits select for distinct sizes of apolar P1-residues. In agreement with structural data,[6] the fluorogenic substrate Ac-WLA-AMC, featuring a P1-Ala side chain can be used to monitor β5c activity.[5] We observed that the IC_{50} value of the P1-Ala compound Ac-LAA-ep for subunit β5c (1.1 μM) is reduced up to 55-fold compared to analogues bearing Leu, Phe, or Tyr as P1 side chains (IC_{50}: < 0.06 μM; Tables 2 and 3). Ac-LAA-ep, however, does not inhibit subunit β5i, and thus it represents a basic scaffold for developing β5c-selective compounds. Crystallographic data disclose that Ala undergoes hydrophobic contacts with Met45 of the yβ5-S1 pocket (Ala C$^{\beta}$ to Met45 C$^{\gamma}$/S: 4 Å) without changing its position (Figure

DOI: 10.1021/jacs.5b03688
J. Am. Chem. Soc. 2015, 137, 7835−7842

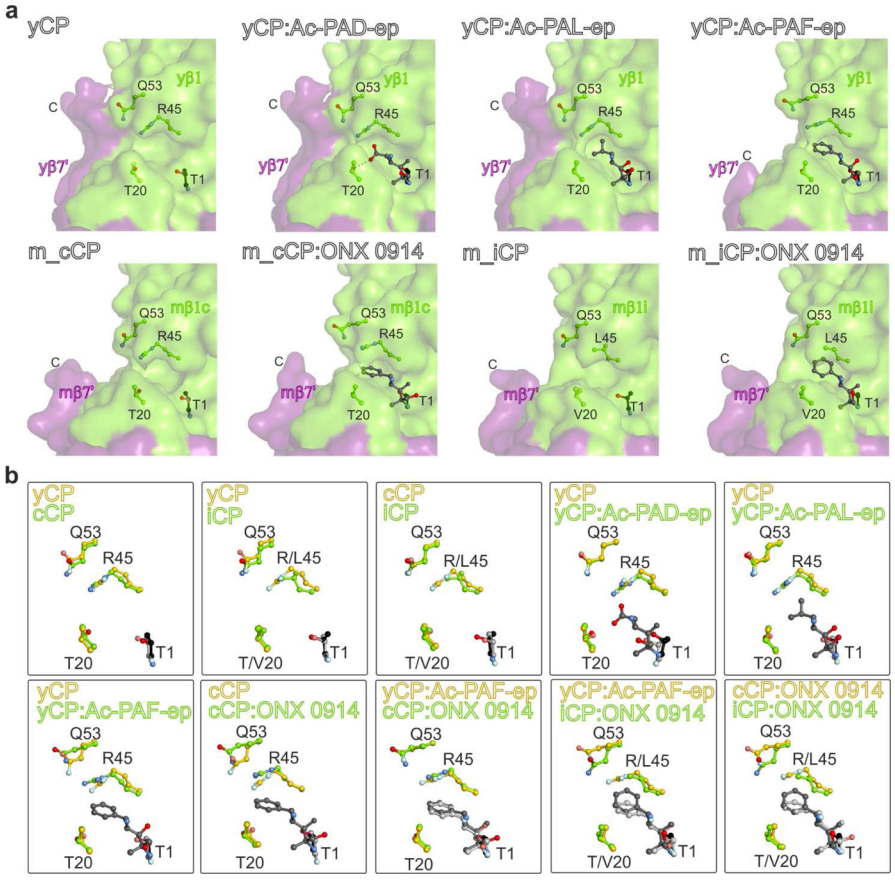

Figure 3. C-terminus of subunit $\beta7$. (a) Surface drawings of the yeast and mouse proteasome subunits $\beta1$ (green) and $\beta7'$ (purple). The $\beta1$ active site residues Thr1, Thr20 ($\beta1c$)/Val20 ($\beta1i$), Arg45 ($\beta1c$)/Leu45 ($\beta1i$), and Gln53 as well as bound ligands are illustrated as balls and sticks. Only the P1 site of ligands (gray) is shown. The y$\beta1$ subunit mediates critical contacts with the C-terminus of $\beta7'$. In yeast, binding of inhibitors bearing phenylalanine in P1 disrupts these interactions, leading to the disorder of the $\beta7'$ C-terminus (upper row of pictures). In the mouse cCP and iCP, such structural changes are absent due to the shorter $\beta7'$ C-terminus. (b) Structural superpositions of the active site residues shown in panel a. In their apo state, y$\beta1$, $\beta1c$, and $\beta1i$ active sites superimpose well. Binding of compounds with P1-Leu or P1-Asp residues to the yCP does not affect the orientation of the $\beta1$ active site residues, whereas docking of P1-Phe shifts the position of Arg45 and Gln53 in the yCP and mouse cCP. Thus, the subunits y$\beta1$ and $\beta1c$ prefer Leu or Asp residues at the P1 position. Notably, binding of ONX 0914 (P1-Phe) to subunit $\beta1i$ does not alter the positions of the residues 45 and 53 (see Figure S4f, Supporting Information).

S3d,g, Supporting Information). The $\beta5i$-S1 site does not provide this stabilization because the peculiar conformation of Met45 enlarges the S1 pocket. Hence, subunit $\beta5i$ is not targeted by Ac-LAA-ep (AlaC$^{\beta}$ to Met45: 5.7−7.4 Å; Figure S3h, Supporting Information).[6]

Fluorogenic substrates for $\beta5c$ and $\beta5i$ feature either Leu or Tyr as P1 residues (carboxybenzyl-Gly-Gly-Leu-para-nitroanilide (Z-GGL-pNA), N-succinyl-Leu-Leu-Val-Tyr-AMC (Suc-LLVY-AMC)[20]), and most inhibitors of the $\beta5$ active site, including the FDA approved drugs bortezomib and carfilzomib, bear Leu in P1. We found that epoxyketones with Leu, Phe, or Tyr in P1 as well as Leu in P3 are very potent inhibitors of both human $\beta5c$ ($IC_{50} \leq 0.1$ μM) and $\beta5i$ ($IC_{50} \leq 1.0$ μM; Table 2) as well as of the yeast counterpart ($IC_{50} \leq 0.72$ μM; Table 3). Structural data visualize that these hydrophobic P1 side chains undergo van der Waals contacts with Ala20, Val31, Met45, and Ala49. In addition, the P1-Tyr can be weakly stabilized by a hydrogen bond between its hydroxyl group and Gln53N$^{\varepsilon}$ of y$\beta5$ and $\beta5i$ (3.0 Å; Figure S3d, Supporting Information). In the $\beta5c$ substrate binding channel, Tyr may hydrogen-bond to Ser53O$^{\gamma}$ ($\beta5c$) and Ser118O$^{\gamma}$ ($\beta6$) as previously proposed,[6] thereby explaining its high affinity for $\beta5c$- and $\beta5i$-subunits. Consistent with previous suggestions,[6,21] the P1-Leu residue drives $\beta5c$ selectivity: Ac-LAL-ep is 17 times more specific for $\beta5c$ than $\beta5i$ (Table 2). The tendency of Ac-LAF-ep to favor $\beta5c$ over $\beta5i$ (up to six times) probably results from the P3 and P2 residues (Table 2). The P3-Leu, which is accepted by both $\beta5c$ and $\beta5i$,[6,14,19,21,22] and the P2-Ala residue, which fails to interact with Cys48 of $\beta5i$, do not promote $\beta5i$ but $\beta5c$ selectivity. Altogether, these results imply that the P1 side chain is a major determinant of affinity for $\beta5$ subunits but does not act as the sole decisive factor.

General Aspects for Targeting $\beta1$. The yeast y$\beta1$ and the mammalian constitutive $\beta1c$ subunits have been attributed to cleave peptide bonds after negatively charged amino acids.[23] To assay this activity of the proteasome, the fluorogenic substrate Z-Leu-Leu-Glu-AMC is frequently used. However, we and others[8,9] found that y$\beta1$ and $\beta1c$ prefer ligands featuring Asp and Leu at P1 over those bearing Glu or any other amino acid in this position (Tables 2 and 3; Figure 2c). For instance, the IC_{50} values of P1-Asp/Leu compounds for $\beta1c$ range ≤ 1.6 μM, whereas those for all other compounds are ≥ 5.3 μM. In agreement, bortezomib (Leu in P1; $IC_{50} \leq 1$ μM) but not ONX 0914 (Phe in P1; $IC_{50} > 10$ μM) targets the subunits y$\beta1$ and $\beta1c$ with high affinity (Tables 2 and 3). The wild-type

DOI: 10.1021/jacs.5b03688
J. Am. Chem. Soc. 2015, 137, 7835−7842

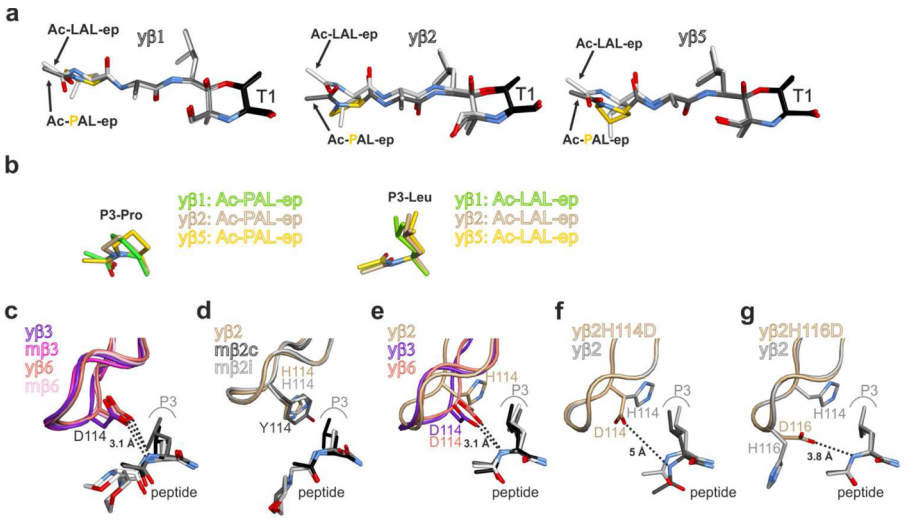

Figure 4. Impact of residue 114 of β2, β3, and β6 on ligand binding. (a) Superposition of the compounds Ac-LAL-ep (light gray) and Ac-PAL-ep (dark gray) bound to the yeast β1, β2, and β5 subunits highlights differences at the P3 site. P3-Pro and P3-Leu featuring compounds adopt almost identical conformations in the yβ1 substrate binding channel, while in the yβ2 and yβ5 counterpart, profound changes are observed. These explain the disfavor of P3-Pro compounds by the latter two active sites. (b) Superposition of the Ac-PAL-ep bound to yβ1 (green), yβ2 (brown), and yβ5 (yellow) depicts subunit-specific differences in the orientation of the P3-Pro residue, whereas for the P3-Leu side chain of Ac-LAL-ep, no significant alterations are observed. (c) Superposition of yeast and mouse β3 and β6 subunits visualize that Asp114 occupies the same position in all subunits. Notably, Asp114 is hydrogen-bonded to the P3 amide nitrogen atom of the ligand's peptide backbone (Ac-LAF-ep for yeast and ONX 0914 for mouse). The P3 sites of ligands are depicted as sticks. (d) Superposition of yeast and mouse β2 subunits indicates that His114 (yβ2 and mβ2i) and Tyr114 (mβ2c) perfectly overlay and lack any interaction with the ligand's peptide backbone. (e) Superposition of the yeast β2, β3, and β6 subunits illustrates that only Asp114 in β3 and β6 hydrogen-bonds to the P3 amide nitrogen atom of the ligand. Notably, the position of the C^{α} atom of His114 in yβ2 significantly deviates from that observed for Asp114 of yβ3 and yβ6. (f) Despite the mutation H114D, subunit β2 fails to hydrogen-bond to the ligand's peptide backbone (distance 5 Å). (g) The mutation yβ2H116D is also unable to stabilize the ligand's peptide backbone by a hydrogen bond (distance 3.8 Å).

yCP:Ac-PAE-ep crystal structure revealed that Glu fits well in the yβ1 S1 pocket (Figure S3a, Supporting Information) but lacks any direct interaction with surrounding protein residues (see also note in Supporting Information). In contrast to Glu, the P1-Asp is hydrogen-bonded to Thr20OH (2.8 Å), and the P1-Leu undergoes favorable van der Waals interactions with the methyl group of Thr20 (3.7 Å). These contacts cause the Asp and Leu side chains to adopt distinct orientations in the S1 pocket. Repulsion of the positively charged Arg45 and the nonpolar P1-Leu side chain is prevented by a negatively charged counterion (e.g., Cl^-) that is hydrogen-bonded to Arg45NH1 and Arg45NH2 (Figure 2a,b). The minor stabilization of the Glu side chain compared to Asp and Leu causes its disfavor at the P1 position. In conclusion, the yβ1 and β1c active sites of the proteasome rather exert C-L and ChT-L than PGPH activities and rather select for a certain size of side chain than for its charge. Regarding potency and selectivity for β1c, Ac-PAD-ep and Ac-LAD-ep are the most outstanding compounds ($IC_{50} \leq 1.6$ μM; Table 2).

Consistent with structural data[3,6] and cleavage pattern analyses,[11] the β1i substrate binding channel is targeted by compounds featuring hydrophobic residues (Table 2). The apolar β1i active site surroundings (e.g., Val20 and Leu45 in β1i versus Thr20 and Arg45 in β1c) enhance the IC_{50} values of Ac-PAL-ep (IC_{50}: 0.11 μM (β1c)/0.028 μM (β1i)) and Ac-LAL-ep (IC_{50}: 0.95 μM (β1c)/0.020 μM (β1i)) at least four-times compared to β1c by providing favorable van der Waals stabilization. Besides Leu, also the aromatic amino acids Phe (IC_{50}: $\geq$ 10.8 μM (β1c)/ $\leq$ 0.23 μM (β1i)) and Tyr (IC_{50}: $\geq$ 5.3 μM (β1c)/ $\leq$ 0.38 μM (β1i)) represent appropriate P1 residues for β1i-ligands. In fact, the respective compounds are up to 500 times more selective for β1i than for β1c (Table 2).[18] We previously supposed that ONX 0914 targets β5i over β1i due to steric hindrance with Phe31 of the β1i S1 pocket.[6] Nonetheless, Phe containing ligands can be used to block subunit β1i.[18]

Next, we evaluated acetyl (Ac)-capped tetra- versus tripeptides and found that elongation of Ac-PLL-ep by a P4-Ala residue enhances the IC_{50} value for yβ1 and β1c by a factor of four (Tables 2 and 3). In addition, Ac-APLL-ep (IC_{50}: 0.029 μM) is 25 times more active for β1c than H-APLL-ep (IC_{50}: 0.72 μM; Table 2). Our structural data visualize that a hydrogen bond between the carbonyl oxygen atom of the acetyl-cap and Thr22OH additionally stabilizes these elongated inhibitors in yβ1 (distance ~3 Å; Figure S3b, Supporting Information). Thr22 is conserved in mammalian β1c subunits but exchanged for Ala in β1i entities. Congruently, the IC_{50} values of Ac-APLL-ep (IC_{50}: 0.035 μM) and H-APLL-ep (IC_{50}: 0.085 μM) for subunit β1i are almost identical. In summary, capped tetrapeptides may be useful to target β1c.

The β7 C-Terminus and Its Impact on Caspase-like Activity. Yeast β1 and mammalian β1c subunits are largely insensitive to inhibitors featuring Phe or Tyr in P1 (IC_{50} > 5 μM; Tables 2 and 3). This disfavor is provoked by the polar S1 pockets of the yβ1/β1c subunits and the structural changes that are triggered upon ligand binding. Particularly, the P1-Phe of ONX 0914 and Ac-P/LAF-ep dislocates Arg45 and Gln53[6] and in yeast additionally disrupts the interactions of yβ1 with the C-terminal tail of subunit yβ7′ of the opposite β′-ring (Figure 3; Figure S4d,e, Supporting Information). This ultimately results in the disorder of up to 11 amino acids of yβ7′ (Table S5, Supporting Information). The C-terminal appendage of subunit β7 is crucial for efficient proteasome assembly in eukaryotes because it governs the association of two half-proteasomes

DOI: 10.1021/jacs.5b03688
J. Am. Chem. Soc. 2015, 137, 7835−7842

during CP biogenesis.[25] Compared with yeast, the β7 C-terminus of mammals is shortened by four amino acids (Figure S4a, Supporting Information).[6,14,25,26] In agreement, binding of the P1-Phe residue of ONX 0914 to the mouse cCP does not induce pronounced structural changes in subunit β7 (Figure 3a).[6] Surprisingly, removal of the C-terminal part of subunit yβ7 interferes with C-L activity (Figure S4b, Supporting Information).[25,27] Crystallographic analyses of this truncation mutant (β7ΔC) demonstrated that all active sites are matured and indistinguishable from wt yCP. Furthermore, the proteolytic centers are susceptible to covalent modification by inhibitors, thereby proving their structural integrity (Figure S4c,d, Supporting Information). These conflicting data (bound ligands versus lack of C-L activity) result from the high concentration of inhibitors used for soaking experiments and indicate that the mutant yCP is functional but maybe less effective for dynamic reasons.

The S3 Pocket—A Peculiarity of the β1 Active Site. P3-Pro ligands serve as potent inhibitors of C-L[8,18] or BrAAP (branched chain amino acid-preferring)[28,29] activities and as selective substrates (e.g., Ac-PAL-AMC) to monitor peptide bond hydrolysis by β1i.[5] The structural basis for the β1-preference of the P3-Pro residue, however, remained elusive.

We analyzed the subunit selectivity profile of various compounds bearing either Leu or Pro residues at their P3 site for the yeast as well as mammalian CPs. In contrast to the β1 active sites, the β2 and β5 subunits disfavor inhibitors with Pro at P3 (Tables 2 and 3). Crystallographic analyses revealed that many epoxyketones with a P3-Pro residue leave subunit yβ2 unmodified even at millimolar concentrations (Table S4, Supporting Information). Furthermore, Ac-LAE-ep and Ac-LAD-ep bind to all active sites of the proteasome, but the corresponding P3-Pro ligands are specific for β1 (Table S4, Supporting Information). Hence, it is the poor affinity of the Pro-ligands for the subunits β2 and β5 that causes their β1 selectivity.

The non-primed substrate binding channels of the proteasome are formed by two adjacent β subunits (β1/2, β2/3, and β5/6), with β2, β3, and β6 contributing to the S3 pockets of the β1, β2, and β5 active sites (Figure 1). For instance, Asp114O$^{\delta}$ of β3 and β6 hydrogen bonds to the amide nitrogen of P3-Leu ligands bound to β2 and β5, respectively (Figure 4c)[3,6,14] and thereby stabilizes the ligand in the substrate binding channel. The backbone nitrogen of P3-Pro compounds, however, is not accessible for this interaction. Furthermore, in β2/3 and β5/6, the P3-Pro inhibitors are shifted compared to the Leu-counterparts (Figures 4a,b) because Asp114 hinders placing of the Pro side chain in the S3 pocket (distance ≥ 3.0 Å). By contrast, P3-Pro and P3-Leu featuring inhibitors adopt the same conformation in β1, which suggests that the structure of the β1/2 substrate binding channel tolerates P3-Pro-residues better than the β2/β3 and β5/β6 active sites.

Indeed, the β1/2 active site is ideally suited to accommodate P3-Pro ligands. Instead of Asp114, β2 encodes either His114 (in yβ2/β2i subunits) or Tyr114 (in β2c subunits). According to the mouse cCP and iCP crystal structures, both Tyr114 in β2c and His114 in β2i and yβ2 adopt the same side chain orientation. However, this conformation clearly differs from that observed for Asp114 in β3 and β6 and prevents hydrogen-bonding to the P3 nitrogen of ligands (Figure 4d,e). Consequently, at the β1/2 active site, P3-Leu ligands are less stabilized, and P3-Pro ones do not receive repulsion.

Most yeast proteasome structures visualize alternative conformations of His114 that may act as a "swinging door" and kink ligands bound to β1/2 compared with β2/3 and β5/6 (Figure S5b, Supporting Information). In addition, around residue 114, the structure of the β2 protein backbone differs from that of the subunits β3 and β6 (Figure 4e). To test (1) whether this unique arrangement in β2 results from His/Tyr114, (2) whether the side chain itself gives rise to the preference for P3-Pro, and (3) whether we can mimic the characteristics of the β2/3 and β5/6 S3 pocket in β1, we substituted yβ2His114 by Asp. We expected this mutation to enhance the affinity for P3-Leu ligands (via hydrogen-bonding of Asp114 to the P3-amide nitrogen of the ligand as observed for β2/3 and β5/6) and to restrict the tolerance of P3-Pro compounds (due to repulsion with Asp114). Surprisingly, the C-L (β1) activity of this mutant was strongly reduced compared with wt yCP, thus preventing reliable determination of IC_{50} values (Figure S5c, Supporting Information). Peptide bond hydrolysis by the β1 active site is commonly monitored by the AMC-substrate Z-LLE-AMC. On the basis of our assumptions and the P3-Leu residue of the substrate used, we assumed to observe wt-like or even increased activity of the yβ2H114D mutant yCP toward Z-LLE-AMC. Structural data demonstrate that the active sites are matured and susceptible to inhibition by epoxyketones (Figure S5d, Supporting Information). The mutation H114D increases the size of the S3 pocket and leads to a more kinked conformation of P3-Leu inhibitors (Figure 4f; Figure S5e, Supporting Information). However, H114D does not change the orientation of the surrounding loop and is therefore located too far apart from the inhibitor for hydrogen-bond formation (5.0−5.8 Å; Figure 4f). This observation conforms to the fact that no enhanced turnover of Z-LLE-AMC was detected for the mutant.

Besides residue 114, the conserved His116 in β2 may account for the tolerance of P3-Pro residues and the bending of tetrapeptides in the β1/β2 substrate binding channel. For instance, carfilzomib is less potent for subunit β1 than β5 because His116 blocks its P4-homophenylalanine moiety.[14,19] We created the mutants yβ2H116N, yβ2H116D, and yβ2H116E and found that the C-L activity of these mutants was also significantly reduced (up to five-fold) compared to wt yCPs, with the mutant yβ2H116D being most affected (Figure S5c, Supporting Information). Nonetheless, ligand complex structures could be obtained for all three mutants. These data illustrate that the inhibitors adopt wt-like conformation (Figure S5d, Supporting Information). Like Asp114, Asp116 is unable to mediate hydrogen-bonding to the P3 backbone nitrogen atom of ligands (distance 3.8 Å; Figure 4g). Elongation of Asp116 by a methylene group to Glu116 was also ineffective due to reorientation of the Glu side chain (distance to P3 backbone nitrogen 5.2−6.0 Å; Figure S5d, Supporting Information).

In summary, we found that introduction of Asp114 or Asp/Glu116 in yβ2 significantly impairs the catalytic activity of the β1 subunit. Consequently, the impact of the mutations on the affinities of P3-Pro versus P3-Leu compounds could not be assessed. The structural data obtained on the mutants suggest that the unique backbone orientation around His114 in subunit yβ2 cannot be altered and that the disfavor of P3-Pro residues by the β2/3 and β5/6 active sites cannot be mimicked in β1/2. Altogether, we conclude that the distinct mammalian substrate specificities cannot be exchanged among the different subunits simply by point mutagenesis.

DOI: 10.1021/jacs.5b03688
J. Am. Chem. Soc. 2015, 137, 7835−7842

CONCLUSION

A series of 23 tri- and tetrapeptide epoxyketone proteasome inhibitors was synthesized. They feature varying P1 residues, including hydrophobic and acidic ones, and bear either a P3-Leu or P3-Pro residue. All compounds were examined for their potency and subunit selectivity in human cell lysates and with purified yeast proteasome. The binding modes of all inhibitors were visualized by X-ray crystallography. The obtained data reveal the following key findings. (1) Epoxyketones featuring Val or Ile as P1 residues are disfavored by yeast and human proteasomes. (2) We identified two compounds that favor the β2c and β5c, respectively, over the i-counterparts: Ac-LAE-ep and Ac-LAA-ep. (3) Yeast and human constitutive β1 active sites prefer Asp over Glu at the P1 position and thus exert rather caspase-like activities. Besides Asp, Leu is also well accepted by the yβ1/β1c S1 pocket. (4) We provide structural explanations for the β1-preference of P3-Pro-featuring compounds. Asp114 of β3 and β6 impairs binding of P3-Pro ligands to the β2 and β5 subunits, while His/Tyr114 of β2 allows their accommodation in the β1/2 substrate binding channel due to exceptional backbone and side chain orientations. Together, the immense amount of structural and biochemical data presented here will support future efforts to improve existing proteasome inhibitors as well as to design proteasome-type selective and subunit-specific drugs. Such compounds would serve to characterize in more detail the biological roles of the individual proteasomal active sites and might qualify for diverse medical applications including cancer and inflammatory diseases.

ASSOCIATED CONTENT

Supporting Information

Figures, tables, experimental procedures, characterization data, mass spectra, and ^{1}H and ^{13}C NMR spectra. The Supporting Information is available free of charge on the ACS Publications website at DOI: 10.1021/jacs.5b03688.

AUTHOR INFORMATION

Corresponding Authors

*h.s.overkleeft@chem.leidenuniv.nl
*michael.groll@tum.de

Author Contributions

[‖]E.M.H. and G.d.B. contributed equally to this work.

Notes

The authors declare no competing financial interest.

ACKNOWLEDGMENTS

The staff of the beamline X06SA at the Paul-Scherrer-Institute, Swiss Light Source, Villigen Switzerland is acknowledged for assistance during data collection. The research leading to these results has received funding from the European Community's Seventh Framework Programme (FP7/2007-2013) under BioStruct-X (grant agreement N°283570). We thank Richard Feicht for the purification and crystallization of yeast 20S proteasomes. This work was supported by the Deutsche Forschungsgemeinschaft (DFG, Grant No. GR1861/10-1) and the SFB 1035/A2.

REFERENCES

(1) Groettrup, M.; Kirk, C. J.; Basler, M. *Nat. Rev. Immunol.* **2010**, *10*, 73.
(2) Murata, S.; Takahama, Y.; Tanaka, K. *Curr. Opin. Immunol.* **2008**, *20*, 192.
(3) Groll, M.; Ditzel, L.; Löwe, J.; Stock, D.; Bochtler, M.; Bartunik, H. D.; Huber, R. *Nature* **1997**, *386*, 463.
(4) Mirabella, A. C.; Pletnev, A. A.; Downey, S. L.; Florea, B. I.; Shabaneh, T. B.; Britton, M.; Verdoes, M.; Filippov, D. V.; Overkleeft, H. S.; Kisselev, A. F. *Chem. Biol.* **2011**, *18*, 608.
(5) Blackburn, C.; Gigstad, K. M.; Hales, P.; Garcia, K.; Jones, M.; Bruzzese, F. J.; Barrett, C.; Liu, J. X.; Soucy, T. A.; Sappal, D. S.; Bump, N.; Olhava, E. J.; Fleming, P.; Dick, L. R.; Tsu, C.; Sintchak, M. D.; Blank, J. L. *Biochem. J.* **2010**, *430*, 461.
(6) Huber, E. M.; Basler, M.; Schwab, R.; Heinemeyer, W.; Kirk, C. J.; Groettrup, M.; Groll, M. *Cell* **2012**, *148*, 727.
(7) Orlowski, M. *Biochemistry* **1990**, *29*, 10289.
(8) Kisselev, A. F.; Garcia-Calvo, M.; Overkleeft, H. S.; Peterson, E.; Pennington, M. W.; Ploegh, H. L.; Thornberry, N. A.; Goldberg, A. L. *J. Biol. Chem.* **2003**, *278*, 35869.
(9) Nussbaum, A. K.; Dick, T. P.; Keilholz, W.; Schirle, M.; Stevanovic, S.; Dietz, K.; Heinemeyer, W.; Groll, M.; Wolf, D. H.; Huber, R.; Rammensee, H. G.; Schild, H. *Proc. Natl. Acad. Sci. U. S. A.* **1998**, *95*, 12504.
(10) Harris, J. L.; Alper, P. B.; Li, J.; Rechsteiner, M.; Backes, B. J. *Chem. Biol.* **2001**, *8*, 1131.
(11) Toes, R. E.; Nussbaum, A. K.; Degermann, S.; Schirle, M.; Emmerich, N. P.; Kraft, M.; Laplace, C.; Zwinderman, A.; Dick, T. P.; Muller, J.; Schonfisch, B.; Schmid, C.; Fehling, H. J.; Stevanovic, S.; Rammensee, H. G.; Schild, H. *J. Exp. Med.* **2001**, *194*, 1.
(12) Nazif, T.; Bogyo, M. *Proc. Natl. Acad. Sci. U. S. A.* **2001**, *98*, 2967.
(13) Groll, M.; Kim, K. B.; Kairies, N.; Huber, R.; Crews, C. M. *J. Am. Chem. Soc.* **2000**, *122*, 1237.
(14) Harshbarger, W.; Miller, C.; Diedrich, C.; Sacchettini, J. *Structure* **2015**, *23*, 418.
(15) Verdoes, M.; Willems, L. I.; van der Linden, W. A.; Duivenvoorden, B. A.; van der Marel, G. A.; Florea, B. I.; Kisselev, A. F.; Overkleeft, H. S. *Org. Biomol. Chem.* **2010**, *8*, 2719.
(16) Li, N.; Kuo, C. L.; Paniagua, G.; van den Elst, H.; Verdoes, M.; Willems, L. I.; van der Linden, W. A.; Ruben, M.; van Genderen, E.; Gubbens, J.; van Wezel, G. P.; Overkleeft, H. S.; Florea, B. I. *Nat. Protoc.* **2013**, *8*, 1155.
(17) Groll, M.; Korotkov, V. S.; Huber, E. M.; De Meijere, A.; Ludwig, A. *Angew. Chem., Int. Ed. Engl.* **2015**, DOI: 10.1002/anie.201502931.
(18) de Bruin, G.; Huber, E. M.; Xin, B. T.; van Rooden, E. J.; Al-Ayed, K.; Kim, K. B.; Kisselev, A. F.; Driessen, C.; van der Stelt, M.; van der Marel, G. A.; Groll, M.; Overkleeft, H. S. *J. Med. Chem.* **2014**, *57*, 6197.
(19) Huber, E. M.; Heinemeyer, W.; Groll, M. *Structure* **2015**, *23*, 407.
(20) Heinemeyer, W.; Kleinschmidt, J. A.; Saidowsky, J.; Escher, C.; Wolf, D. H. *EMBO J.* **1991**, *10*, 555.
(21) Huber, E. M.; Groll, M. *Angew. Chem., Int. Ed. Engl.* **2012**, *51*, 8708.
(22) Demo, S. D.; Kirk, C. J.; Aujay, M. A.; Buchholz, T. J.; Dajee, M.; Ho, M. N.; Jiang, J.; Laidig, G. J.; Lewis, E. R.; Parlati, F.; Shenk, K. D.; Smyth, M. S.; Sun, C. M.; Vallone, M. K.; Woo, T. M.; Molineaux, C. J.; Bennett, M. K. *Cancer Res.* **2007**, *67*, 6383.
(23) Orlowski, M.; Wilk, S. *Arch. Biochem. Biophys.* **2000**, *383*, 1.
(24) Löwe, J.; Stock, D.; Jap, B.; Zwickl, P.; Baumeister, W.; Huber, R. *Science* **1995**, *268*, 533.
(25) Ramos, P. C.; Marques, A. J.; London, M. K.; Dohmen, R. J. *J. Biol. Chem.* **2004**, *279*, 14323.
(26) Unno, M.; Mizushima, T.; Morimoto, Y.; Tomisugi, Y.; Tanaka, K.; Yasuoka, N.; Tsukihara, T. *Structure* **2002**, *10*, 609.
(27) Hilt, W.; Enenkel, C.; Gruhler, A.; Singer, T.; Wolf, D. H. *J. Biol. Chem.* **1993**, *268*, 3479.
(28) Cardozo, C.; Vinitsky, A.; Michaud, C.; Orlowski, M. *Biochemistry* **1994**, *33*, 6483.
(29) Orlowski, M.; Cardozo, C.; Michaud, C. *Biochemistry* **1993**, *32*, 1563.

DOI: 10.1021/jacs.5b03688
J. Am. Chem. Soc. 2015, 137, 7835−7842